ACADÉMIE
DES SCIENCES
INSTITUT DE FRANCE

# Comptes Rendus

# Mécanique

Fakhreddine Bouali, Semchedine Fedala, Hugo André and Ahmed Felkaoui

**Intelligent bearing faults diagnosis in non-stationary conditions based on angular resampling and support vector machine**

Volume 353 (2025), p. 499-518

Online since: 20 March 2025

https://doi.org/10.5802/crmeca.292



CENTRE
MERSENNE

*The* Comptes Rendus. Mécanique *are a member of the*
*Mersenne Center for open scientific publishing*
www.centre-mersenne.org — e-ISSN : 1873-7234

ACADÉMIE
DES SCIENCES
INSTITUT DE FRANCE

*Comptes Rendus. Mécanique*
**2025**, Vol. 353, p. 499-518
https://doi.org/10.5802/crmeca.292

Research article / *Article de recherche*

# Intelligent bearing faults diagnosis in non-stationary conditions based on angular resampling and support vector machine

## *Diagnostic intelligent des défauts de roulements en conditions non stationnaires basé sur le rééchantillonnage angulaire et les machines à vecteurs de support*

**Fakhreddine Bouali** [*, a], **Semchedine Fedala** [a], **Hugo André** [b] and **Ahmed Felkaoui** [a]

[a] Laboratory of Applied Precision Mechanics, Institute of Optics and Precision Mechanics, Ferhat Abbes University Setif 1, Setif 19137, Algeria

[b] Université de Lyon, Université Jean Monnet de Saint-Etienne, LASPI EA3059, 20 Avenue de Paris, 42334 Roanne, France

*E-mail:* bouali.f@univ-setif.dz (F. Bouali)

**Abstract.** Over the past decades, intelligent bearing diagnostic methods have become a research hotspot. These methods require the construction of a Feature Vector (FV) generally composed of indicators calculated from time sampled vibration signals. However, in non-stationary conditions, these signals require the application of complex methods whose calculation time is really important. For this reason, the use of angular resampling techniques is recommended because they make it possible to get rid of speed fluctuations and to employ simple processing methods.

In this work, we propose to use angularly resampled acceleration signals for intelligent bearing fault diagnosis under non-stationary conditions. It is the question of comparing three types of FV: classic angular indicators on angular signals $x(\theta)$, original order spectrum indicators (peak amplitude), or the combination of the two previous families of indicators. Then, the selection phase is performed by the Minimum Redundancy Maximum Relevance (MRMR) algorithm to select the most relevant features. Finally, the classification is carried out by a cubic support vector machine (SVM) for the detection and identification stages of various bearings fault conditions. The effectiveness of the proposed method achieves a perfect classification rate of 100%.

**Résumé.** Au cours des dernières décennies, les méthodes intelligentes de diagnostic des roulements sont devenues un sujet de recherche majeur. Ces méthodes nécessitent la construction d'un vecteur forme (VF), généralement composé d'indicateurs calculés à partir de signaux de vibration échantillonnés à pas de temps constant. Cependant, en conditions non stationnaires, ces signaux exigent l'application de méthodes complexes, dont le temps de calcul est particulièrement élevé. C'est pourquoi l'utilisation des techniques de rééchantillonnage angulaire est recommandée, car elles permettent de s'affranchir des fluctuations de vitesse et d'employer des méthodes de traitement plus simples.

* Corresponding author

Dans ce travail, nous proposons d'utiliser des signaux d'accélération rééchantillonnés angulairement pour le diagnostic intelligent des défauts de roulements en conditions non stationnaires. Il s'agit de comparer trois types de vecteurs formes : des indicateurs angulaires classiques sur les signaux angulaires $x(\theta)$, des indicateurs spectraux d'ordre originaux (amplitude de pic) ou la combinaison de ces deux familles d'indicateurs. Ensuite, la phase de sélection est réalisée à l'aide de l'algorithme *Minimum Redundancy Maximum Relevance* (MRMR) afin de choisir les indicateurs les plus pertinents. Enfin, la classification est effectuée par la méthode machine à vecteurs de support cubique (SVM Cubique) pour les étapes de détection et d'identification des différentes conditions de défaut des roulements. L'efficacité de la méthode proposée permet d'atteindre un taux de classification parfait de 100 %.

**Keywords.** Bearings, Fault diagnosis, Support vector machines, Time-varying rotating speed, Angular resampling.

**Mots-clés.** Roulements, Diagnostic des défauts, Machines à vecteurs de support, Vitesse de rotation variable, Rééchantillonnage angulaire.

**Funding.** Algerian Ministry of Higher Education and Scientific Research (PNE 2019–2020).

*Manuscript received 23 December 2024, revised 27 February 2025, accepted 1 March 2025.*

## 1. Introduction

The complicated form of machines in modern industry makes their faults diagnosis more complex. Bearings are the most commonly used elements in these machines and their failure is known as the main causes of machine breakdowns. Effective bearing faults diagnosis plays a very important role in preventing faults and increasing machine disponibility and reliability. Research has focused on the detection and diagnosis of bearing faults, intending to increase the accuracy and speed of calculation, reducing costs, performing real-time monitoring and diagnosis, and improve the efficiency of repair and troubleshooting, which has resulted in the use of machine learning algorithms (MLA) to automatically diagnose faults in rotating machinery [1,2]. Previous research have proven the performance of many MLA in bearing diagnosis such as the K-Nearest Neighbors (KNN) [3], Gaussian process [4], Hidden Markov Model (HMM) [5,6], and Bayesian Neural Networks (BNN) [7], These non-parametric methods are based on the probability laws and require a large number of samples i.e. several features vectors (FV), leading to a problem of storage and computational costs. Unlike most classification methods, the Support Vector Machine (SVM) does not require a large number of training samples to solve a learning problem [8]. Another popular classification method called Artificial Neural Networks (ANN) incorporates recursive algorithms that adjust system parameters based on a risk function such as empirical risk minimization (ERM) during the training process. Nevertheless, this method requires a relatively large number of samples to perform the learning of the different classes. However, the SVM uses a risk function known as structural risk minimization (SRM) which allows the algorithm to take data sparseness into account and minimize the upper bound error of an expected risk [9].

The construction of the Features Vectors (FV) is a primary task. Each FV is composed of indicators that must be able to define the different operating modes, thus reflecting the exact meaning of the classes that represent the different operating states [10,11]. Before calculating the features, it is necessary to pre-process the signals. Various signal processing techniques suitable for bearing faults diagnosis such as Fourier transform or envelope analysis have been widely studied. The latter aims at demodulating HF band expected to carry bearing fault signature, since the signal induced by a bearing defect excites the high resonance frequencies. Therefore, automatic determination of the optimal demodulation band is often necessary [12]. For this, Spectral Kurtosis (SK) is a useful technique designed to determine the optimal demodulation-band automatically [13,14]. However, for varying speed conditions, the previous methods are unable to detect the defects. So, different time-frequency analysis techniques have been established to eliminate the influence of speed variation [15], Huang et al. proposed Empirical Mode Decomposition (EMD) to solve the problem of non-stationary conditions [16]. Although it presents some drawbacks such as the lack of mathematical formulation and the mode mixing under singularities [17]. Researchers have proposed new methods to adjust these problems. For instance, Smith proposed the Local Mean Decomposition (LMD) [18], Ziani et al. proposed the EMD, TKO and Shock Detector to diagnose gears faults in non-stationary conditions [19], and the Local Characteristic scale Decomposition (LCD) was introduced by Cheng et al. [20]. Other methods based on the exploitation of the Amplitude and Frequency Modulation property (AM-FM) of the Intrinsic Mode Function (IMF) have been proposed to obtain a rigorous mathematical formulation and better robustness to noise compared to EMD method like the Empirical Wavelet Transform (EWT) [21], the Variational Mode Decomposition (VMD) [22] and the Adaptive Local Iterative Filtering (ALIF) [23]. Thus, all these Adaptive Mode Decomposition (AMD) methods share the same disadvantage, which makes them only suitable to analyze signals without spectral overlap. Whereas, Order Analysis (OA) is considered to be the most widely used method for detecting bearing faults under variable speed conditions. This method transforms the vibration signal from the time domain to the angular domain by resampling it at a constant angle interval using interpolation [24,25]. These angular signals have the particularity of ensuring an integer constant number of samples per revolution and thus eliminate the effects of speed variations. Several techniques are used in the literature for the angular resampling of vibration signals [10,26,27].

In this study, we propose to demonstrate the effectiveness of angularly resampled acceleration signals in the intelligent diagnosis of bearing faults operating only under non-stationary conditions. It is a question to show how to extract relevant indicators to build a feature vector from the angular signals. Thus, we compare three FVs types: the first is composed only from the classic angular indicators on angular signals $x(\theta)$, the second is composed only from the order spectrum indicators (peak amplitude), and the last is the combination of both previous families of indicators. Then, to select the most relevant features, the Minimum Redundancy Maximum Relevance (MRMR) algorithm is applied. Finally, the classification is carried out by a cubic support vector machine (Cubic SVM) for the stages of bearing fault detection and identification.

The layout of this paper is as follows: Section 2 introduces the principle of angular resampling. In Section 3 we outline the classification procedure by SVM. Section 4 is devoted to the description of the database. Section 5 describes the proposed algorithm, the obtained results and discussions. Finally, Section 6 concludes this paper.

## 2. Angular resampling

Generally, temporal vibration signals are the most used in the field of rotating machinery monitoring despite their sensitivity to non-stationary conditions [25]. However, angular resampling eliminates the effects of speed variations since it ensures a constant number of points per period. There are several techniques for obtaining angular signals [26,27]. The angular resampling technique is an interesting alternative to direct angular sampling because it does not require expensive instrumentation and also offers the possibility to exploit both temporal and angular signals. This technique can rely on the simultaneous recording of vibration and encoder signals. Then, the angular acceleration signal is obtained through the interpolation of the vibration signal at each angular position delivered by the encoder [10].

Figure 1 presents the angular resampling method. The technique consists in determining the angular positions $\Delta\theta(i)$ $i = 1,2,\ldots,n$ according to the rising edges appearance time $\Delta t(i)$ $i = 1,2,\ldots,n$ of the encoder pulse. Then, the resampling of the temporal signal in the angular domain is performed by cubic "spline" interpolation [28]. Algorithm 1 summarizes the steps of the angular resampling used in this study using zero crossing method.

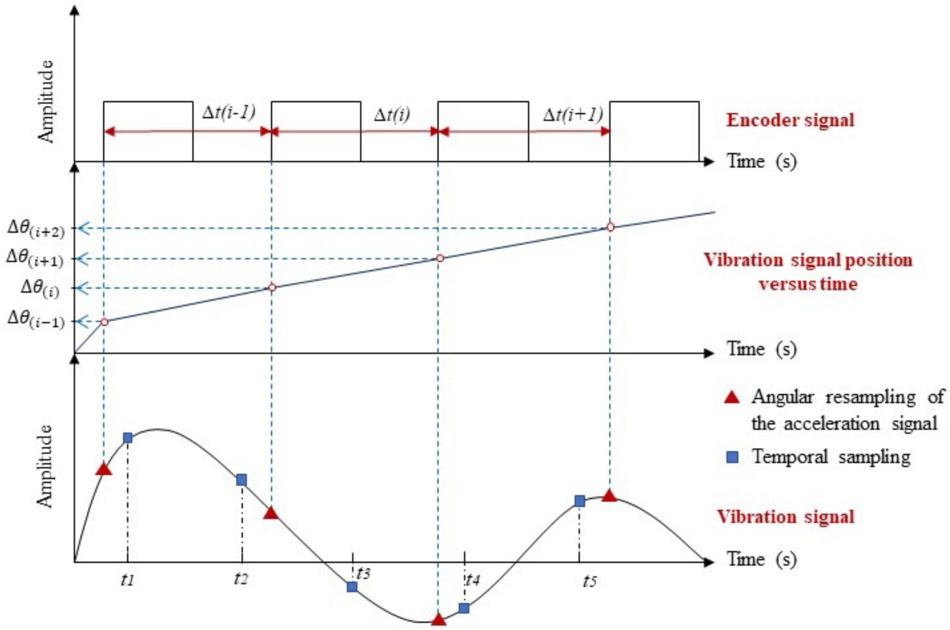


**Figure 1.** Angular resampling.

| **Algorithm 1:** Angular resampling using a zero-crossing | | |
|---|---|---|
| **Input** | $x(t_i), F_s$, *Resolution, TTL signal* | |
| **Procedure** | *Step 1* | Determine the low and high states of the encoder signal |
| | *Step 2* | Find the times at which each pulse starts ($t_i$) |
| | *Step 3* | Determine the time intervals between pulse ($\Delta t_i$) |
| | *Step 4* | Estimate: "angle time" function |
| | *Step 5* | Determine $\Delta\theta_i$ |
| | *Step 6* | Cubic interpolation of $x(t_i)$ at $x(\theta_i)$ |
| **Output** | $x(\theta_i)$ | |

## 3. Classification procedure by SVM method

SVM is a powerful classification tool that is widely used in various machine-learning applications [29–31], SVM's basic principle is to separate two classes using an ideal hyperplane that maximizes the margin between the two hyperplanes. Figure 2 summarizes the basic principle.

To describe the SVM algorithm, let's consider the set P that trains the SVM classifier:

$$P = (x_i, y_i), \quad x_i \in R^m, \quad y_i \in \{-1, 1\}_{i=1}^{n} \quad i = 1, 2, \ldots, n. \tag{1}$$

In the case of linearly separated data, where $x$ an input space containing $m$ indicators of a $n$ training set samples, while $y_i$ is the desired output, and $\begin{cases} y_i = 1 \\ y_j = -1 \end{cases}$ the separating hyperplane $f(x) = 0$. can be presented as:

$$f(x) = w^T x + b = \sum_{i=1}^{n} w_i x_i + b = 0 \tag{2}$$

where $b$ is the bias scalar and $w$ is a weight vector.

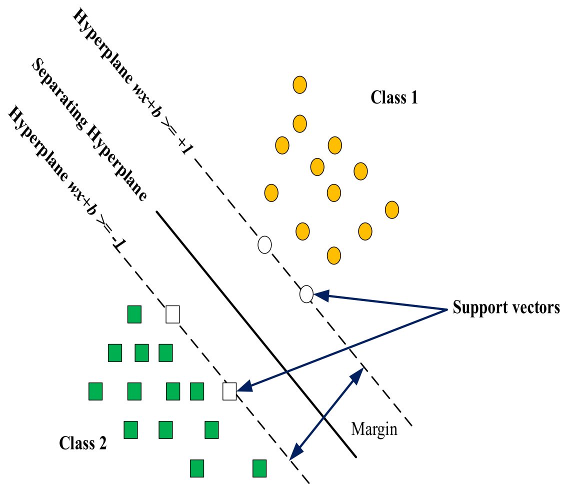


**Figure 2.** An example of two classes separated by SVM.

The hyperplane was defined as:

$$y_i f(x_i) = y_i(w^T x_i + b) - 1 \geq 1. \tag{3}$$

Soft margin are obtained by introducing a slack factor $\xi_i \geq 0$:

$$y_i(w^T x_i + b) \geq 1 - \xi_i \quad (i = 1, 2, \ldots, n). \tag{4}$$

The following equations derived from a soft margin method may be calculated to produce the hyperplane separating the two classes with the maximum distance of $2/\|w\|$ is equivalent to minimizing $\|w\|^2$ from the Euclidean $1/\|w\|$ further to hyperplane $f(x) = 0$.

$$\text{minimise}\left(\frac{1}{2}\|w\|^2 + C\sum_{i=1}^{n}\xi_i\right) \tag{5}$$

where $C$ is the regularization parameter that controls the trade-off between the classification accuracy and the evaluation of the margin maximization.

To overcome the constraints complexity induced by the slack variable, the Lagrangian method (Equation (5)) makes the problem easily solvable and can be extendible to the kernel SVM

$$\text{maximize} W(\alpha) = \sum_{i=1}^{n}\alpha_i - \frac{1}{2}\sum_{ij=1}^{n}\alpha_i\alpha_j y_i y_j (x_i x_j) \tag{6}$$

$\alpha$: Lagrange multiplier.

The kernel function $K$ is used in the case of nonlinear separability to transform the input vectors in to a high dimensional space with linear separability. Where, $(x_i, x_j)$ is replaced by $K(x_i x_j)$.

$$\text{maximize} W(\alpha) = \sum_{i=1}^{n}\alpha_i - \frac{1}{2}\sum_{ij=1}^{n}\alpha_i\alpha_j y_i y_j K(x_i x_j). \tag{7}$$

The optimal classification function can be given:

$$f(x) = \text{sign}\left(\sum_{ij=1}^{n}\alpha_i y_i K(x_i x_j) + b\right) \tag{8}$$

Originally, SVMs were created for binary classes. But many real problems have more than two classes. Multi-class SVMs is an extension of the binary SVM classification issue as described by Wong et al. [32]. Two multi-class SVMs methods, frequently employed are:

**Table 1.** Structural parameters and CDFs of the tested bearings (ER16K)

| Bearing type | Pitch diameter (mm) | Ball diameter (mm) | Number of balls | BPFI | BPFO | BSF |
|---|---|---|---|---|---|---|
| ER16K | 38.52 | 7.94 | 9 | $5.43 \times fr$ | $3.57 \times fr$ | $2.32 \times fr$ |

BPFI: Ball Pass Frequency Inner race, BPFO: Ball Pass Frequency Outer race, BSF: Ball (roller) Spin Frequency, *fr*: Rotating Frequency.

- One-Against-One method (OAO), involves binary SVM classifier construction for all pairs of classes.
- One-Against-All method (OAA), separates each class from all others and constructs a combined classifier.

Hsu et al. [33] compared the multi-class SVMs techniques in detail on major experimental problems, noting that an OAO method is a competitive and effective approach.

In bearing fault classification, several defects like inner race defect, outer race defect, and ball defect occur during fault diagnosis. However, in the case of simultaneous fault conditions, a reliable diagnosis may be more difficult. There may be circumstances when some defects remain stable while others get severe. A robust SVM that can effectively distinguish between healthy and faulty conditions, is thus required, also identifying the severity of damaged fault conditions. In this paper, SVM method is applied to evaluate the impact of angular measurements in an intelligent bearing condition monitoring strategy and accurately and reliably give the presence of specific defective bearing and can also distinguish different types of defects [34].

## 4. Description of the dataset

In this study, we chose the bearing experiment data provided by the University of Ottawa [35] and openly available in [36], for several reasons. First, the instrumentation of this database is inexpensive. Second, the signals are sampled temporally with a very high sampling rate of 200 kHz. Third, the diversity of physical quantities measured (vibration, speed (encoder)). These offer the possibility of applying several advanced signal processing methods and consequently extracting more information on the health status of the system regardless of the operating conditions (types of faults and/or speed variation) and thus validating the effectiveness of the proposed algorithm for non-stationary and general operating.

The experimental setup shown in Figure 3, is performed on a SpectraQuest machinery fault simulator (MFS-PK5M), consisting of a shaft supported on two ball bearings (ER16K) and controlled by an AC drive. Table 1 summarizes the geometric parameters and the Characteristic Defect Frequency (CDFs) of the tested bearings. The healthy bearing is on the left, while the experimental bearing is on the right with different health conditions, Healthy (H), faulty with an Inner Race Defect (IRD), faulty with an Outer Race Defect (ORD), faulty with Ball Defect (BD) and faulty with Combined Defects (CD). An incremental encoder (EPC model 775) with 1024 cycles per revolution measures the shaft rotational speed. In addition, an ICP accelerometer (Model 623C01) was mounted on the housing bearing to obtain vibration signals.

The data are acquired by the NI data acquisition board (NI USB-6212 BNC). Each sampled dataset contains two channels, "Channel_1" is the vibration data and "Channel_2" is the rotational speed data (TTL signals). In all the experiments, vibration and speed signals are sampled at 200 kHz for 10 s for each one. Signals are obtained in four time-varying rotating speed conditions: increasing speed, decreasing speed, increasing then decreasing speed, and decreasing then increasing speed.

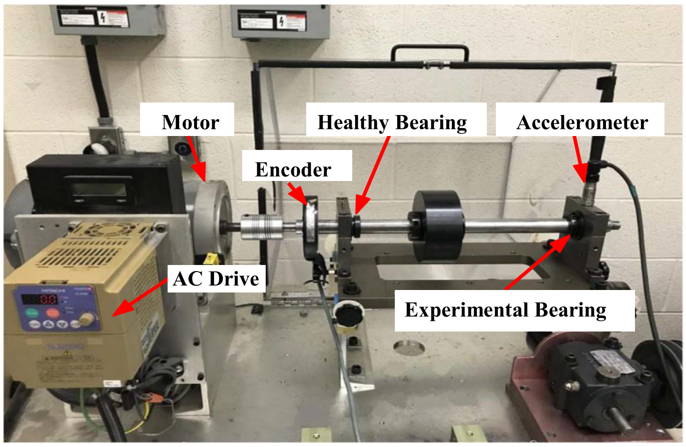


**Figure 3.** Experimental set-up [35].

**Table 2.** Dataset numbering

| Bearing health conditions | Speed varying conditions | | | |
|---|---|---|---|---|
| | Increasing speed | Decreasing speed | Increasing then decreasing speed | Decreasing then increasing speed |
| Healthy | H-A-1<br>H-A-2<br>H-A-3 | H-B-1<br>H-B-2<br>H-B-3 | H-C-1<br>H-C-2<br>H-C-3 | H-D-1<br>H-D-2<br>H-D-3 |
| Faulty (inner race defect) | I-A-1<br>I-A-2<br>I-A-3 | I-B-1<br>I-B-2<br>I-B-3 | I-C-1<br>I-C-2<br>I-C-3 | I-D-1<br>I-D-2<br>I-D-3 |
| Faulty (outer race defect) | O-A-1<br>O-A-2<br>O-A-3 | O-B-1<br>O-B-2<br>O-B-3 | O-C-1<br>O-C-2<br>O-C-3 | O-D-1<br>O-D-2<br>O-D-3 |
| Faulty (ball defect) | B-A-1<br>B-A-2<br>B-A-3 | B-B-1<br>B-B-2<br>B-B-3 | B-C-1<br>B-C-2<br>B-C-3 | B-D-1<br>B-D-2<br>B-D-3 |
| Faulty (combined defect) | C-A-1<br>C-A-2<br>C-A-3 | C-B-1<br>C-B-2<br>C-B-3 | C-C-1<br>C-C-2<br>C-C-3 | C-D-1<br>C-D-2<br>C-D-3 |

Table 2 shows how the dataset is numbered for the following experimental conditions: health and varying speed conditions, for each experimental setting, three trials are obtained, totaling 60 datasets, for example, the dataset H-A-1 presents the vibration and TTL data collected from a healthy bearing and an increased operating rotational speed from 14.1 Hz to 29 Hz. The dataset O-D-3 presents the vibration and TTL data collected from a faulty bearing with an outer race defect and a decreasing operating rotational speed from 25.5 Hz to 15 Hz, then increasing to 19.6 Hz. The description of the other datasets is detailed in [35].

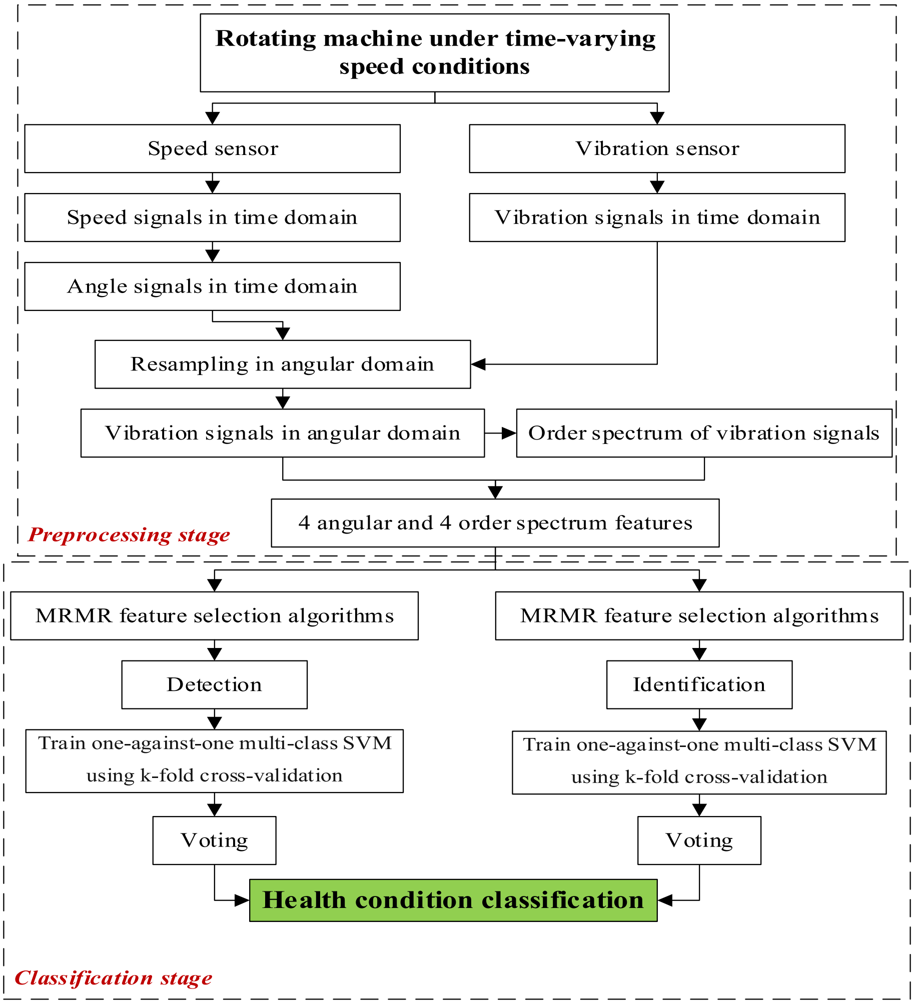


**Figure 4.** Proposed method flowchart.

## 5. Experimental part

Figure 4 shows the flowchart of the methodology employed in this study. The encoder signals are used to resample vibration signals in the angular domain. Then, different types of indicators are extracted to construct three FVs. The first is composed from four classic angular indicators. The second FV is composed from four order spectrum indicators. The last is the combination of the previous FVs. All FVs will then be used to train and test the SVM classifiers without and with selection using the MRMR algorithm. The classification is divided in two stages. First, the detection stage is carried out by testing the Healthy (H) class with the Damaged class (D). Second, the identification is performed to compare only all damaged classes (IRD, ORD, BD, and CD).

### 5.1. *Signal analysis*

To analyze bearing fault signals under non-stationary conditions, angular resampling is necessary to eliminate speed variation influence. We calculated the following indicators on the angular

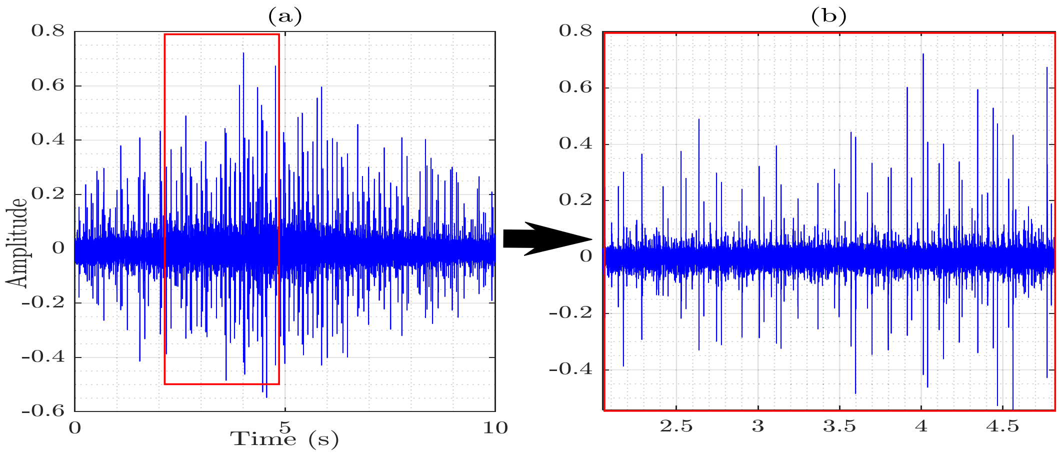


**Figure 5.** (a) Faulty bearing temporal signal with a CD, (Rotation speed increasing then decreasing), (b) The zoomed portion of the signal indicated by a red box.

signals ($x_i$): RMS, kurtosis, Crest Factor (CF), Impulse Factor (IF) [37,38]. The following equations present the mathematical formulas of the obtained indicators respectively:

$$x_{\text{rms}} = \sqrt{\frac{1}{N}\sum_{i=1}^{N}(x_i - \overline{x})^2} \tag{9}$$

$$x_{\text{kurt}} = \frac{\sum_{i=1}^{N}(x_i - \overline{x})^4}{\left[\frac{1}{N}\sum_{i=1}^{N}(x_i - \overline{x})^2\right]^2} \tag{10}$$

$$\text{CF} = \frac{\max|x_i - \overline{x}|}{x_{\text{rms}}} \tag{11}$$

$$\text{IF} = \frac{\max|x_i - \overline{x}|}{\frac{1}{N}\sum_{i=1}^{N}|x_i|}. \tag{12}$$

Figure 5 shows the acceleration signal of the CD, for increasing speed then decreasing. The presence of defects causes a significant increase in temporal signals energy and a presence of random shocks. From this representation, we cannot determine the faults type of this bearing. On the other hand, due to the variation of rotational speed, the periodic pulses cannot be defined in time domain signals. Therefore, it is impossible to judge the presence of a defect or identify its type.

The angular resampling of the vibration signal in an integer number of samples per revolution allows it possible to solve the problems of periodicity and to overcome blurring effect induced by the speed variation. Figure 6 presents the angular signal of the CD, with increasing then decreasing speed conditions. One can easily notice the presence of periodic shocks as well as a significant increase in amplitude compared to the temporal signal (Figure 5).

## 5.2. *Order spectrum analysis*

Order spectrum analysis has proven to be one of the most useful techniques in CM for all rotating machines. Additionally, the Power Spectral Density (PSD) is a highly helpful technique used to detect faults in rotating machines [39]. Many time windows have been developed to minimize

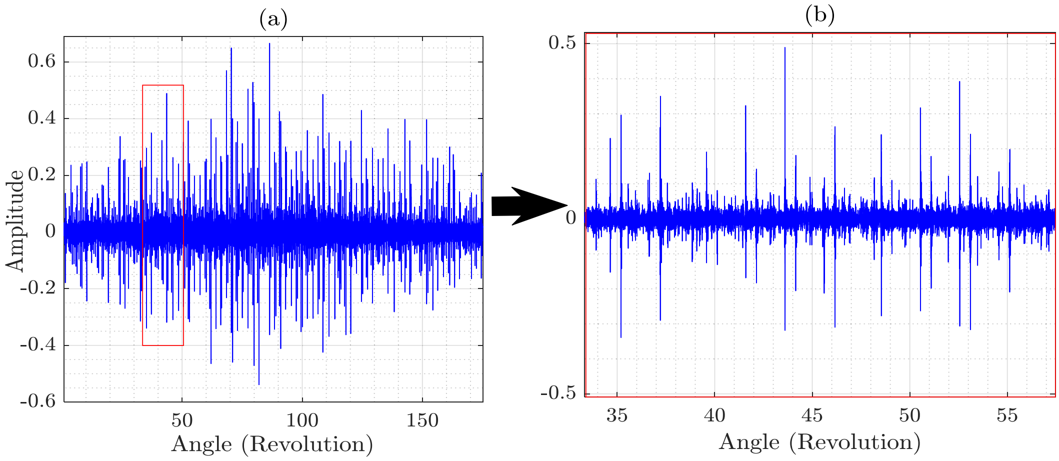


**Figure 6.** (a) Faulty bearing angular signal with a CD, (Rotation speed increasing then decreasing), (b) The zoomed portion of the signal indicated by a red box.

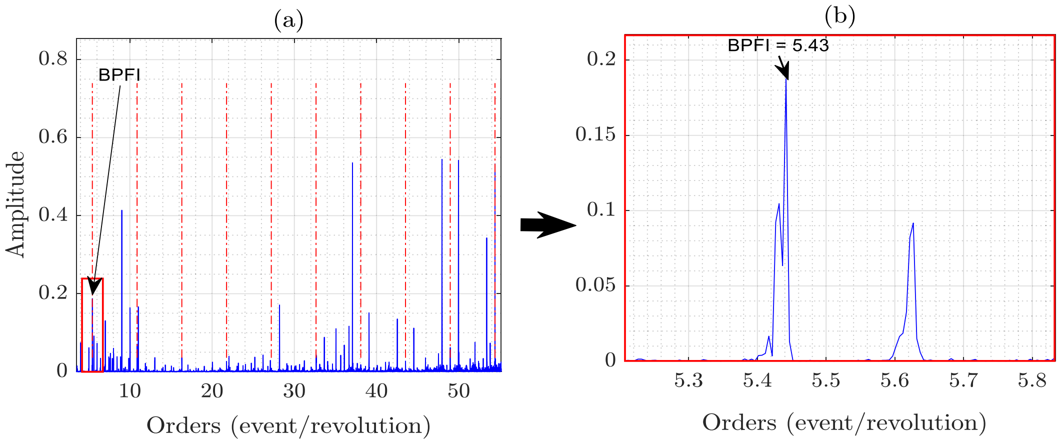


**Figure 7.** (a) Angular signal PSD presentation with Inner Race Defect (Rotation speed increasing from 12.5 Hz to 27.8 Hz), (b) The zoomed portion of the signal indicated by a red box.

the spectral leakage problem induced by PSD. The Hanning window is the most used in spectral analyzes [40]. This window should be adopted as a norm because it provides a good balance between amplitude accuracy and frequency resolution, which minimizes transient errors in periodic repetitions of the time signal [41], and help to minimize the edge effect by reducing the side lobes in the frequency domain.

In this study, we have applied the PSD on an integer number of revolutions, to extract features from the spectrum domain, using the Hanning window, whose length is equal to the length of the signal.

Figure 7 presents the angular signal PSD in the case of IRD, with rotation speed increasing from 12.5 Hz to 27.8 Hz. The BPFI is directly observed in the 5.43 order and its harmonics, which causes a periodic phenomenon and a significant increase in the fault peak amplitude. We note that this fault is the most dominant on the signal in the different fault conditions.

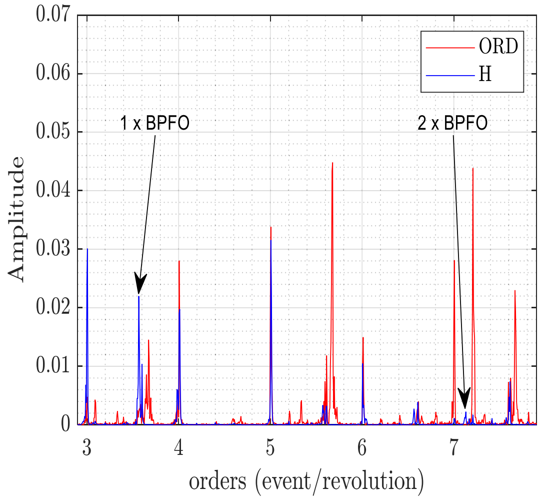


**Figure 8.** Angular signal PSD presentation with ORD (Rotation speed increasing from 14.8 Hz to 27.1 Hz).

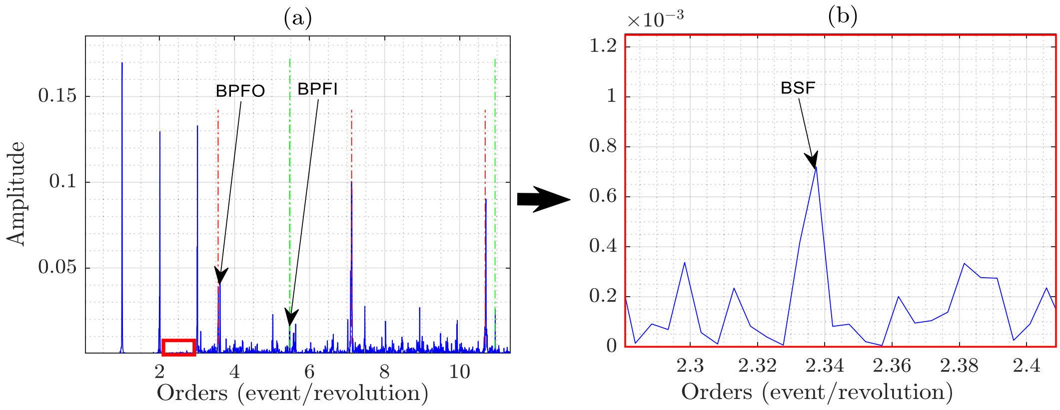


**Figure 9.** (a) Angular signal PSD presentation with CD (Rotation speed increasing from 13 Hz to 27.9 Hz). (b) The zoomed portion of the signal indicated by a red box.

Figure 8 shows the order spectrum of the signal with an ORD. The peak corresponding to this defect is located at order 3.57, which is the fundamental characteristic frequency (BPFO). The energy of the first harmonic in the healthy case (H) is greater than this case (ORD) for all signals, although we took the same number of points for all database signals before the construction of the order spectrum indicators. Many researches discussed this phenomenon, it can be explained by the theory of the "healing phenomenon" when the defect is well advanced [42–45].

Figure 9 shows the angular signal PSD for CD. We distinguish the presence of orders 3.57 and 5.43 corresponding to the outer race (BPFO) and the inner race defects (BPFI) respectively. It can be seen that the inner race fault (BPFI), presents a significant increase in the main order levels and that some of its harmonics are modulated by the shaft rotation. This defect can be considered among the most intensive defect. However, the order spectrum focused on the rotational frequency of the ball at order 2.32 does not clearly show the presence of the defect, we notice a modest increase in amplitude compared to the healthy state (Figure 10).

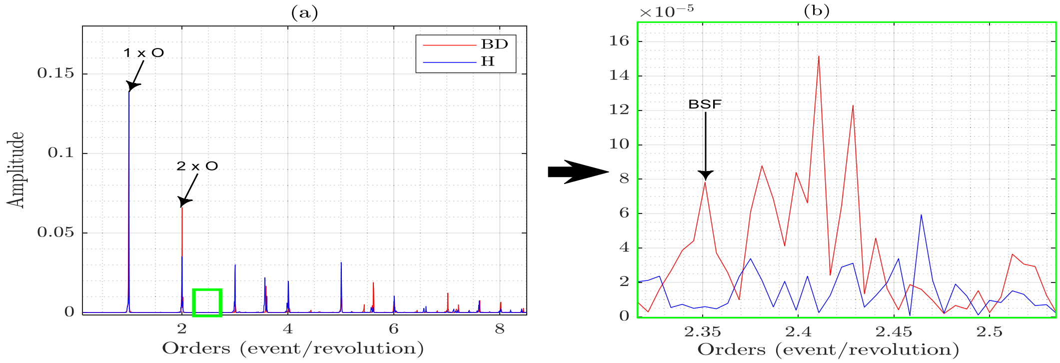


**Figure 10.** (a) Angular signal PSD presentation with BD (Rotation speed increasing from 13 Hz to 27.9 Hz). (b) The zoomed portion of the signal indicated by a green box.

The precedent figures allow a possibility to keep track with precision of the order components of the powers associated with the various conditions, whether a healthy state, inner race defect, outer race defect, a ball defect, or combined defects.

Several approaches have been developed for automating the detection of bearings defects, for example, Shiroishi et al. [46], proposed three frequency domain features: Spectrum peak Ratio Outer (SPRO), Spectrum Peak Ratio Inner (SPRI), and Spectrum Peak Ratio Rolling element (SPRR) to identifying bearing defects. These indicators proved their effectiveness only in stationary conditions. Farhat et al. [47], adapted the precedent features for the angular field using the envelope order analysis technique to eliminate the speed variation. The updated features: SPROa, SPRIa, and SPRRa are obtained by dividing the sum of the defect peaks (fundamental and harmonics) by the sum of all peaks in the order spectrum. This method takes a long computational cost to extract the features. However, the first harmonic of a defect in the order spectrum is sufficient to detect the defect in the bearing.

In this work we propose to use only the level of the first harmonic for each frequency defect, the Level of Inner Race Frequency Defect (LIRFD), the Level of Outer Race Frequency Defect (LORFD), and the Level of Ball Frequency Defect (LBFD), we also take the Sum of the levels of the 40th first harmonics of Orders (SO) as an indicator, because the majority of the bearing faults generating a modulation effect [12]. Renaudin et al. [48] found that the positions of these peaks will remain fixed despite variations in speed, whereas the amplitudes vary differently from one frequency channel to another. In addition, this indicator does not require a long computation time. We employed a computer equipped with an Intel(R) Core (TM) i7-10750H CPU, running on Windows 11 Pro (version 24H2), with 16.0 GB of RAM to construct the Feature Vectors (FVs). To evaluate the computational efficiency of our methodology, we measured the time required for both angular resampling and extracting all indicators. For a single signal, the entire process was completed in less than 0.2 s. When processing the entire database, the total computational time was under 18 s. These results highlight the efficiency and speed of the proposed method, confirming its suitability for real-time applications and high-dimensional time series data analysis. Furthermore, the results demonstrate that the proposed method outperforms techniques found in the literature source for bearing defect diagnosis under various conditions, such as those based on time-frequency features extracted through Wavelet Packet Transform (WPT) and dimension reduction using Multi-Weight Singular Value Decomposition (MWSVD), where the reduced dimensionality features are used in Support Vector Machines (SVM) for bearing fault diagnosis [49]. This performance advantage is attributed

**Table 3.** Features description

| Indicators | Domain | H | IRD | ORD | BD | CD |
|---|---|---|---|---|---|---|
| 1 | Angular | RMS | | | | |
| 2 | | Kurtosis | | | | |
| 3 | | Crest Factor (CF) | | | | |
| 4 | | Impulse Factor (IF) | | | | |
| 5 | Spectrum | LIRFD | | | | |
| 6 | | LORFD | | | | |
| 7 | | LBFD | | | | |
| 8 | | SO | | | | |

to the method's ability to efficiently handle complex datasets while maintaining computational tractability.

## 5.3. *Feature vectors (FVs) construction*

One of the most vital steps in the pattern recognition process is feature vector construction. The objective of this step is twofold: firstly, the reduction of the dimensionality of the data provided to the classifier while keeping the maximum information relating to the different classes of functioning. Secondly, converting vibration signals into monitoring indicators which enables a more efficient use of classification [50].

From the angular signals cited in the previous section, we calculated 8 indicators which are summarized in Table 3. In total, 3 FVs were constructed from different domains in order to determine the one that provides the best classification performance in the bearing fault detection and identification stage. The three FVs used are:

- FV composed from the angular domain indicators
- FV composed from the order spectrum domain indicators
- FV composed from a mixture of angular and order spectrum domain indicators.

To keep the same order of magnitude and the same physical units, all FVs are normalized with center 0 and standard deviation 1 using the standard MATLAB function "normalize" specified with a "z-score" option.

## 5.4. *Feature selection by MRMR algorithm*

Feature selection has been widely studied in areas such as machine learning, pattern recognition, data mining, and signal processing. Selected features are used to reduce the data dimensionality by choosing an optimal subset of features that increases classification accuracy. Regarding class/label classification, the challenge is to find the feature subset with the lowest cardinality that maintains the information found in the whole feature set $X = \{X^{(1)}, X^{(2)}, \ldots, X^{(d)}\}$ with class set $C = \{c_1, c_2, \ldots, c_m\}$. The two most common feature selection techniques are filters and wrappers [51]. Filters approaches are the most used because they quantify intrinsic feature values such as feature variance, feature relevance and also take reduced computation time compared to wrapper methods. Consequently, we propose to apply a filter type selection method called MRMR algorithm which means Minimum Redundancy Maximum Relevance Algorithm. This method uses the mutual information of predictor variables and response variables (Equation (13)) to identify an optimal collection of mutually and maximally different features in order to maximize the relevance of a set of features with respect to the response variable [52,53].

The mutual information $I$ of the discrete random variables $X$ and $Z$ is defined as:

$$I(X,Z) = \sum_{i,j} P(X = x_i, Z = z_j) \log \frac{P(X = x_i, Z = z_j)}{P(X = x_i), P(Z = z_j)} \tag{13}$$

where $I = 0$ if $X$ and $Z$ are independent, and $I$ equal $X$ entropy if $X$ and $Z$ are both random variables.

The MRMR is used to identify an optimal set $S$ of features that maximizes the relevance $V_S$ of $S$ for a response variable y, and reduces the redundancy $W_S$ of $S$.

Using $I$, $V_S$ and $W_S$ are expressed in the following Equations (14) and (15):

$$V_S = \frac{1}{|S|} \sum_{x \in S} I(x,y) \tag{14}$$

$$W_S = \frac{1}{|S|^2} \sum_{x,z \in S} I(x,z) \tag{15}$$

$|S|$ presents the number of features in $S$.

The MRMR algorithm uses the Mutual Information Quotient (MIQ) value Equation (16) to rank features via the forward addition scheme which requires $O(|\Omega| \cdot |S|)$ calculations. Where $\Omega$ is the full feature set and $S$ is the optimal set.

$$\mathrm{MIQ}_x = V_x / W_x \tag{16}$$

$V_x$ and $W_x$ are the relevance and redundancy of a feature:

$$V_x = I(x,y) \tag{17}$$

$$W_x = \frac{1}{|S|} \sum_{z \in S} I(x,z). \tag{18}$$

The MRMR algorithms rank features as follows:

(1) Select the feature with $\max_{x \in \Omega} V_x$ and insert the selected indicator into an empty set $S$.
(2) Find the features in the complement of $S$, $S^c$. That have nonzero relevance and zero redundancy. If $S^c$ lacks a feature with nonzero relevance and zero redundancy, go to step 4. Otherwise, choose the feature that is most relevant $\max_{x \in S^c, W_x = 0} V_x$.
(3) Repeat Step 2 until the redundancy for all features in $S^c$ is not zero.
(4) Select the feature in $S^c$ with the largest MIQ value, nonzero relevance, and nonzero redundancy, and add it to the set $S$.

$$\max_{x \in S^c} \mathrm{MIQ}_x = \max_{x \in S^c} \frac{I(x,y)}{\frac{1}{|S|} \sum_{z \in S} I(x,z)} \tag{19}$$

(5) Repeat Step 4 until the significance for all features in $S^c$ is zero.
(6) In a random pattern, add the features without relevance to $S$.

The MRMR selection algorithm is applied to select the best indicators from the combined FV to verify that the combination of classic angular and order spectrum indicators improves the performance of the classification. Table 4 presents the ranked indicators for the detection and identification stages. In the detection stage, it can be observed that the spectral indicators LIRFD and LORFD are the most relevant indicators, while the crest factor and the LBFD are ranked third and fourth indicator respectively. The other indicators are ranked in the last positions. In the identification stage, the five relevant indicators are respectively the RMS, SO, LORFD, kurtosis, and LIRFD. The rest of indicators listed in order of relevance are: IF, LBFD and CF. From these results, one can logically suppose that the combination of classic angular and order spectrum indicators gives the best classification performance because the classic indicators allow to follow the general health state of the machine which allows to easily detect the presence of an anomaly, while the spectral indicators offer the identification of the fault type and origin, thus we confirm the result gives by the Mohanty reference in [38].

**Table 4.** Ranked features

| Indicator rank | Detection | Identification |
|---|---|---|
| 1 | LIRFD | RMS |
| 2 | LORFD | SO |
| 3 | Crest Factor (CF) | LORFD |
| 4 | LBFD | Kurtosis |
| 5 | Kurtosis | LIRFD |
| 6 | Impulse Factor (IF) | Impulse Factor (IF) |
| 7 | RMS | LBFD |
| 8 | SO | Crest Factor (CF) |

**Table 5.** SVM classification performances without selection

| Domain | | |
|---|---|---|
| Angular | FV (04 indicators) | |
| | | Success (%) |
| | Detection | 90 |
| | Identification | 93.8 |
| Order spectrum | FV (04 indicators) | |
| | Detection | 93.3 |
| | Identification | 89.6 |
| Angular & order spectrum | FV (08 indicators) | |
| | Detection | **98.3** |
| | Identification | **97.9** |

## 5.5. *Results and discussions*

We have different types of faults, so it is essential not only to detect but also to identify these faults. For this, a cubic SVM classifier is used for each of the two diagnostic stages. The detection stage, where the data set is split into two classes, the healthy and damaged conditions. The classification in this stage is performed using a 5-fold Cross-Validation (CV). The identification stage in which the data set consists only of faulty operating cases (4 classes). Here, we applied the One-Against-One approach for multi-class classification using a 4-fold CV. In total, $N(N-1)/2$ classifiers are built and each one trains the data of two classes ($N$ is the number of classes). The Cross-Validation Accuracy (CVA) is obtained by averaging the $k$ individual accuracies:

$$\mathrm{CVA} = 1/k\sum_{j=1}^{k} A_j \tag{20}$$

where $k$ (4 in our case) is the number of folds used, and $A_j$ is the accuracy measure of each fold, $j = 1,\ldots,k$.

Table 5 illustrates the classification performance for the three FVs: angular, spectral, and combined FV (angular and spectral). It can be noted that the best classification performance is obtained using the combined FV with a success percentage of 98.3% for the detection stage and 97.9% for the identification stage. While the performances obtained with the other two FVs are lower. For the angular FV, the performances reach 90% for the detection stage and 93.8% for the identification stage. For the spectral FV, the classification performance is equal to 93.3% for the detection stage and 89.6% for the identification stage.

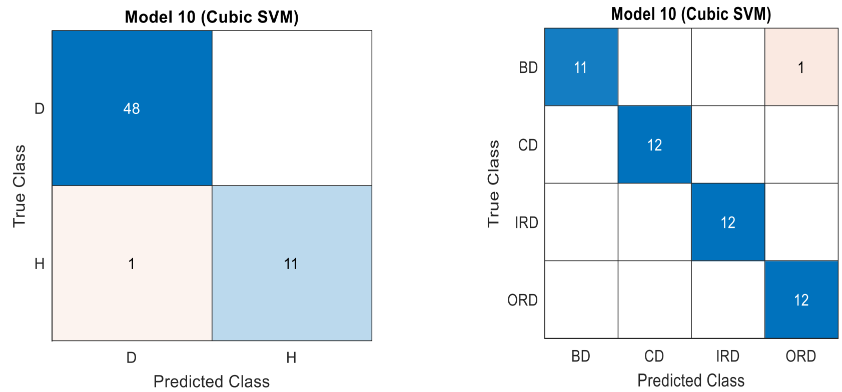


(a) Detection stage (b) Identification stage

**Figure 11.** Confusion matrices of combined FV.

**Table 6.** SVM classification performances with MRMR selection algorithm

| Domain | | | |
|---|---|---|---|
| Angular & spectral | Detection | Success (%) | **100** |
| | | Number of selected indicators | 7 |
| | Identification | Success (%) | **100** |
| | | Number of selected indicators | 4 |

The confusion matrices of the detection and identification stages using the combined FV are displayed in Figures 11a,b respectively. It can be seen that in both stages only one sample was misclassified. It is a sample of healthy class which is classified in faulty class for the detection stage and a sample of ball defect class which is classified with outer race fault class for the identification stage.

Table 6 indicates the SVM classifier performances after feature selection of the combined FV using the MRMR algorithm. The classification rate achieves a 100% for the detection and identification stages using only 7 and 4 indicators respectively.

Figures 12a,b show the confusion matrices of the detection and identification stages using the combined FVs after feature selection. It can be seen that all the samples are well classified which gives perfect performance for detecting and identifying the bearing faults.

The results of the previous section demonstrate that the proposed algorithm can accurately distinguish between different bearing fault conditions especially in non-stationary conditions.

In the preprocessing step, the angular resampling of the vibration signals shows several advantages. Firstly, it eliminates the shift of the spectrum induced by the speed variation. Moreover, it delivers the same number of points per revolution contrary to time signals in non-stationary conditions, which keeps the angular acceleration homogeneity. The angular resampling is also effective in minimizing noise in the vibration signals. Thus, it will improve the relevance of monitoring indicators.

In the classification step, the proposed spectral indicators (LIRFD, LORFD, LBFD, SO) show their effectiveness compared to other features used in the literature as said by Farhat et al., in the referenceh [47]. The performance obtained is 93.3% for the detection step and 89.6% for the

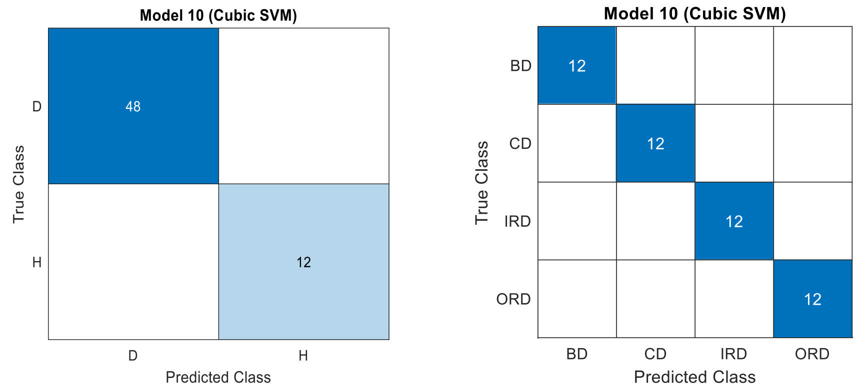


(a) Detection stage (b) Identification stage

**Figure 12.** Confusion matrices of combined FV after features selection.

identification step. Moreover, the classic angular indicators used (RMS, kurtosis, IF, CF) have almost the same classification results as those achieved with the spectral indicators.

The combination of angular and spectral features in one FV increases the performance of the classification for the two stages of detection and identification with 98.3% and 97.9% of success respectively. This combination of indicators exploits the information complementarity because the statistical features are effective for monitoring the machine's health state and spectral domain features are effective for fault location. The MRMR feature selection algorithm allows to have a perfect classification performance with 100% of success and also minimizes the size of FV which reduces significantly computational costs.

## 6. Conclusion

In this research, we propose a new intelligent bearing fault diagnosis method in non-stationary conditions based on angular resampling of acceleration signals and SVM.

In the signal preprocessing step, the acceleration signals are angularly resampled using the speed signals delivered by an incremental encoder. The instants corresponding to each angular position are determined by cubic interpolation. In the FV construction step, we used four classic angular indicators (RMS, Kurtosis, IF, CF) and we proposed four indicators calculated from the order spectrum (LIRFD, LORFD, LBFD and SO). In the classification step, the SVM is trained to classify the defect categories for the detection and identification stages using three different FVs. The first is calculated from the angular domain, the second is extracted from the order spectrum domain, to take advantage of the information complementarity we have combined the two FVs in one FV.

The results indicate that the angular resampling leads to more relevant indicators and combining these features increases classification performance to reach approximately 98%. On the other hand, the MRMR selection algorithm allows the reduction of the FV size which has a double advantage. Firstly, the classification performances will achieve 100% accuracy for the detection and identification stages. Secondly, the computation time of the classification algorithm will be reduced. The proposed method proves its efficiency for bearing fault diagnosis in variable speed conditions. Moreover, this approach will be tested on more complex systems operating under non-stationary conditions, such as wind turbine gearboxes and also this method could be used to build an online diagnostic system.

## Data availability statement

Data that support the findings of this study are available in a public, open access repository: Mendeley Data, V2, doi:10.17632/v43hmbwxpm.2. Huang, Huan; Baddour, Natalie (2019), "Bearing Vibration Data under Time-varying Rotational Speed Conditions".

## Declaration of interests

The authors do not work for, advise, own shares in, or receive funds from any organization that could benefit from this article, and have declared no affiliations other than their research organizations.

## Acknowledgments

This work was achieved at the laboratories LMPA (IOMP, Sétif -1- University, Algeria) and LASPI (Lyon University, France). The authors would like to thank the Algerian Ministry of Higher Education and Scientific Research for their financial and technical support in the framework of the program PNE 2019–2020. A thought and a great recognition for Dr. Hafida Mahgoun who contributed extremely and rigorously at the beginning of the project and who unfortunately deceased before the completion of this work.

## References

[1] Q. Wang, R. Huang, J. Xiong, J. Yang, X. Dong, Y. Wu, Y. Wu and T. Lu, "A survey on fault diagnosis of rotating machinery based on machine learning", *Meas. Sci. Technol* **35** (2024), no. 10, article no. 102001.

[2] S. Manikandan and K. Duraivelu, "Fault diagnosis of various rotating equipment using machine learning approaches—a review", *Proc. Inst. Mech. Eng. E: J. Process Mech. Eng.* **235** (2021), no. 2, pp. 629–642.

[3] H. S. Kumar and G. Upadhyaya, "Fault diagnosis of rolling element bearing using continuous wavelet transform and K-nearest neighbour", *Mater. Today: Proc.* **92** (2023), pp. 56–60.

[4] W. J. Lee and J. W. Sutherland, "Time to failure prediction of rotating machinery using dynamic feature extraction and gaussian process regression", *Int. J. Adv. Manuf. Technol.* **130** (2024), no. 5, pp. 2939–2955.

[5] E. Soave, G. D'Elia and G. Dalpiaz, "Prognostics of rotating machines through generalized Gaussian hidden Markov models", *Mech. Syst. Signal Process.* **185** (2023), article no. 109767.

[6] W. Shuhui, X. Jiawei, Z. Yongteng and Z. Yuqing, "Convolutional neural network-based hidden markov models for rolling element bearing fault identification", *Knowl.-Based Syst.* **144** (2018), pp. 65–76.

[7] G.-J. Jiang, J.-S. Yang, T.-C. Cheng and H.-H. Sun, "Remaining useful life prediction of rolling bearings based on Bayesian neural network and uncertainty quantification", *Qual. Reliab. Eng. Int.* **39** (2023), no. 5, pp. 1756–1774.

[8] Z. K. Abdul and A. K. Al-Talabani, "Highly accurate gear fault diagnosis based on support vector machine", *J. Vib. Eng. Technol.* **11** (2023), no. 7, pp. 3565–3577.

[9] B.-S. Yang, T. Han and W.-W. Hwang, "Fault diagnosis of rotating machinery based on multi-class support vector machines", *J. Mech. Sci. Technol.* **19** (2005), no. 3, pp. 846–859.

[10] S. Fedala, D. Rémond, R. Zegadi and A. Felkaoui, "Contribution of angular measurements to intelligent gear faults diagnosis", *J. Intell. Manuf.* **29** (2018), pp. 1115–1131.

[11] R. Ziani, A. Felkaoui and R. Zegadi, "Bearing fault diagnosis using multiclass support vector machines with binary particle swarm optimization and regularized Fisher's criterion", *J. Intell. Manuf.* **28** (2017), pp. 405–417.

[12] R. B. Randall and J. Antoni, "Rolling element bearing diagnostics—a tutorial", *Mech. Syst. Signal Process.* **25** (2011), no. 2, pp. 485–520.

[13] J. Antoni, "The spectral kurtosis: a useful tool for characterising non-stationary signals", *Mech. Syst. Signal Process.* **20** (2006), no. 2, pp. 282–307.

[14] H. Li, X. Wu, T. Liu and S. Li, "Rotating machinery fault diagnosis based on typical resonance demodulation methods: a review", *IEEE Sens. J.* **23** (2023), no. 7, pp. 6439–6459.

[15] L. Dongdong, L. Cui and H. Wang, "Rotating machinery fault diagnosis under time-varying speeds: a review", *IEEE Sens. J.* **23** (2023), no. 24, pp. 29969–29990.

[16] N. E. Huang, Z. Shen, S. R. Long, et al., “The empirical mode decomposition and the Hilbert spectrum for nonlinear and nonstationary time series analysis”, *Proc. R. Soc. Lond. A* **454** (1998), no. 1971, pp. 903–995.

[17] Z. Wu and N. E. Huang, “A study of the characteristics of white noise using the empirical mode decomposition method”, *Proc. R. Soc. Lond. A* **460** (2004), no. 2046, pp. 1597–1611.

[18] J. S. Smith, “The local mean decomposition and its application to EEG perception data”, *J. R. Soc. Interface R. Soc.* **2** (2005), no. 5, pp. 443–454.

[19] R. Ziani, A. Hammami, F. Chaari, A. Felkaoui and M. Haddar, “Gear fault diagnosis under non-stationary operating mode based on EMD, TKEO, and shock detector”, *C. R. Mec.* **347** (2019), no. 9, pp. 663–675.

[20] J. Zheng, J. Cheng and Y. Yang, “A rolling bearing fault diagnosis approach based on LCD and fuzzy entropy”, *Mech. Mach. Theory* **70** (2013), pp. 441–453.

[21] D. S. Ramteke, A. Parey and R. B. Pachori, “A new automated classification framework for gear fault diagnosis using fourier–bessel domain-based empirical wavelet transform”, *Machines* **11** (2023), no. 12, article no. 1055.

[22] Y. Guo, Y. K. Ho, X. Zhao, C. Zhang and S. Long, “An IGSA-VMD method for fault frequency identification of cylindrical roller bearing”, *Proc. Inst. Mech. Eng. Part C: J. Mech. Eng. Sci.* **238** (2024), no. 18, pp. 9307–9320.

[23] A. Cicone, J. Liu and H. Zhou, “Adaptive local iterative filtering for signal decomposition and instantaneous frequency analysis”, *Appl. Comput. Harmon. Analysis* **41** (2016), no. 2, pp. 384–411.

[24] M. Zhao, J. Lin, X. Wang, Y. Lei and J. Cao, “A tacho-less order tracking technology for large speed variations”, *Mech. Syst. Signal Process.* **40** (2013), no. 1, pp. 76–90.

[25] D. Remond, “Practical performances of high-speed measurement of gear transmission error or torsional vibrations with optical encoders”, *Meas. Sci. Technol.* **9** (1998), no. 3, pp. 347–353.

[26] H. André, Z. Daher, J. Antoni and D. Remond, “Comparison between angular sampling and angular resampling methods applied on the vibration monitoring of a gear meshing in non stationary conditions”, in *Proceedings of the International Conference on Noise and Vibration Engineering: ISMA2010 including USD2010, Leuven, Belgium*, Curran Associates, Inc., 2010, pp. 2727–2736.

[27] F. Bonnardot, M. E. Badaoui, R. B. Randall, J. Danière and F. Guillet, “Use of the acceleration of a gearbox in order to perform angular resampling (with limited speed fluctuation)”, *Mech. Syst. Signal Process.* **19** (2005), no. 4, pp. 766–785.

[28] K. R. Fyfe and E. D. S. Munck, “Analysis of computed order tracking”, *Mech. Syst. Signal Process.* **11** (1997), no. 2, pp. 187–205.

[29] W. Yin, H. Xia, X. Huang, J. Zhang and M. E. Miyombo, “A fault diagnosis method for nuclear power plant rotating machinery based on adaptive deep feature extraction and multiple support vector machines”, *Progr. Nucl. Energy* **164** (2023), article no. 104862.

[30] L. Lan, X. Liu and Q. Wang, “Fault detection and classification of the rotor unbalance based on dynamics features and support vector machine”, *Meas. Control* **56** (2023), no. 5–6, pp. 1075–1086.

[31] J. Zhang, Q. Zhang, X. Qin and Y. Sun, “A two-stage fault diagnosis methodology for rotating machinery combining optimized support vector data description and optimized support vector machine”, *Measurement* **200** (2022), article no. 111651.

[32] W.-T. Wong and S.-H. Hsu, “Application of SVM and ANN for image retrieval”, *Eur. J. Oper. Res.* **173** (2006), no. 3, pp. 938–950.

[33] C.-W. Hsu and C.-J. Lin, “A comparison of methods for multi-class support vector machines”, *IEEE Trans. Neural Netw.* **13** (2002), no. 2, pp. 415–425.

[34] S. Fedala, D. Rémond, R. Zegadi and A. Felkaoui, “Gear fault diagnosis based on angular measurements and support vector machines in normal and nonstationary conditions”, in *Advances in Condition Monitoring of Machinery in Non-Stationary Operations. CMMNO 2014. Applied Condition Monitoring* (F. Chaari, R. Zimroz, W. Bartelmus and M. Haddar, eds.), Springer International Publishing: Cham, 2015, pp. 291–308.

[35] H. Huang and N. Baddour, “Bearing vibration data collected under time-varying rotational speed conditions”, *Data in Brief* **21** (2018), pp. 1745–1749.

[36] H. Huang and N. Baddour, *Bearing Vibration Data under Time-varying Rotational Speed Conditions*, University of Ottawa: Canada, 2019.

[37] A. Boulenger and C. Pachaud, *Diagnostic Vibratoire en Maintenance Préventive*, Dunod: Paris, 1998.

[38] A. R. Mohanty, *Machinery Condition Monitoring, Principles and Practices*, CRC Press/Taylor & Francis Group: Boca Raton, 2014.

[39] A. A. Mohammed, R. D. Neilson, W. F. Deans and P. MacConnell, “Crack detection in a rotating shaft using artificial neural networks and PSD characterisation”, *Meccanica* **49** (2014), pp. 255–266.

[40] J. Antoni and J. Schoukens, “A comprehensive study of the bias and variance of frequency-response-function measurements : Optimal window selection and overlapping strategies”, *Automatica* **43** (2007), no. 10, pp. 1723–1736.

[41] A. Brandt, *Noise and Vibration Analysis: Signal Analysis and Experimental Procedures*, John Wiley & Sons, Ltd: Chichester, 2011.

[42] T. Williams, X. Ribadeneira, S. Billington and T. Kurfess, "Rolling element bearing diagnostics in run-to-faillure lifetime testing", *Mech. Syst. Signal Process.* **15** (2001), no. 5, pp. 979–993.

[43] M. Buzzoni, J. Antoni and G. D'Elia, "Blind deconvolution based on cyclostationarity maximization and its application to fault identification", *J. Sound Vib.* **432** (2018), pp. 569–601.

[44] H. Qiu, J. Lee, J. Lin and G. Yu, "Wavelet filter-based weak signature detection method and its application on rolling element bearing prognostics", *J. Sound Vib.* **289** (2006), no. 4–5, pp. 1066–1090.

[45] A. Had and K. Sabri, "A two-stage blind deconvolution strategy for bearing fault vibration signals", *Mech. Syst. Signal Process.* **134** (2019), article no. 106307.

[46] J. Shiroishi, Y. Li, S. Liang, T. Kurfess and S. Danyluk, "Bearing condition diagnostics via vibration and acoustic emission measurments", *Mech. Syst. Signal Process.* **11** (1997), no. 5, pp. 693–705.

[47] M. H. Farhat, X. Chiementin, F. Chaari, F. Bolaers and M. Haddar, "Order-based identification of bearing defects under variable speed condition", *Appl. Sci.* **11** (2021), no. 9, article no. 3962.

[48] L. Renaudin, F. Bonnardot, O. Musy, J. B. Doray and D. Rémond, "Natural roller bearing fault detection by angular measurement of true instantaneous angular speed", *Mech. Syst. Signal Process.* **24** (2010), no. 7, pp. 1998–2011.

[49] Z. Huibin, H. Zhangming, W. Juhui, W. Jiongqi and Z. Haiyin, "Bearing fault feature extraction and fault diagnosis method based on feature fusion", *Sensors* **21** (2021), no. 7, article no. 2524.

[50] T. W. Rauber, E. M. do Nascimento, E. D. Wandekokem, F. M. Varejão and A. Herout, "Pattern recognition based fault diagnosis in industrial processes: review and application", in *Pattern Recognition Recent Advances* (A. Herout, ed.), IntechOpen: Rijeka, 2010, pp. 483–508. ISBN: 978-953-7619-90-9.

[51] R. Kohavi and G. H. John, "Wrapper for feature subset selection", *Artif. Intell.* **97** (1997), no. 1–2, pp. 273–324.

[52] G. A. Darbellay and I. Vajda, "Estimation of the information by an adaptive partitioning of the observation space", *IEEE Trans. Inform. Theory* **45** (1999), no. 4, pp. 1315–1321.

[53] C. Ding and H. Peng, "Minimum redundancy feature selection from microarray gene expression data", *J. Bioinform. Comput. Biol.* **3** (2005), no. 2, pp. 185–205.